Chinese Journal of Aeronautics 24 (2011) 265-278

Contents lists available at ScienceDirect

Chinese Journal of Aeronautics

journal homepage: www.elsevier.com/locate/cja

# Bifurcation in a 3-DOF Airfoil with Cubic Structural Nonlinearity

Saied IRANI*, Hamid SARRAFZADEH, Mohammad Reza AMOOZGAR

*Department of Aerospace Engineering, K.N. Toosi University of Technology, Tehran 19697, Iran*

Received 27 September 2010; revised 12 November 2010; accepted 4 March 2011

**Abstract**

Limit cycle oscillations (LCOs) as well as nonlinear aeroelastic analysis of a 3-DOF aeroelastic airfoil motion with cubic restoring moments in the pitch degree of freedom are investigated. Aeroelastic equations of an airfoil with control surface in an incompressible potential flow are presented in the time domain. The harmonic balance (HB) method is utilized to calculate the LCO frequency and amplitude for the airfoil. Also the semi-analytical method has revealed the presence of stable and unstable limit cycles, along with stability reversal in the neighborhood of a Hopf bifurcation. The system response is determined by numerically integrating the governing equations using a standard Runge-Kutta algorithm and the obtained results are compared with the HB method. Also the results by the third order HB (HB3) method for control surface are consistent with the other numerical solution. Finally, by combining the numerical and the HB methods, types of bifurcation, be it supercritical, subcritical, or divergent flutter area are identified.

*Keywords:* flutter; bifurcation; cubic nonlinearity; limit cycle oscillations; harmonic balance method

## 1. Introduction

Aeroelasticity is defined as the interaction of aerodynamics, elasticity and dynamics. The aeroelastic results under the assumption of structural linearity, may disagree with the physical phenomena as most real structures may have structural nonlinearities such as mathematical (freeplay, bilinear and cubic) and physical (friction and hysteresis) nonlinearities. When some nonlinearity assumptions are made, the aeroelastic characteristics of the system particularly after the linear flutter speed could be predictable.

Diversion from linearity comes from aerodynamic and structural nonlinearity where aerodynamic nonlinearities at transonic speeds or high angles of attack may emerge. Structural nonlinearity is classified as being either distributed or concentrated. Distributed structural nonlinearity is governed by elastodynamic deformations that affect the whole structure. Concentrated nonlinearity commonly arises from worn hinges of the control surfaces, loose control linkages, and material strength and resistance, or is related to material behavior.

Limit cycle oscillations (LCOs) and bifurcations arising from a concentrated structural nonlinearity in the restoring forces were first studied by Woolston[1] and Shen[2], et al. Breitbach[3] described the flutter analysis of an airplane with multiple structural nonlinearity in the control system. Laurenson, et al.[4] studied flutter of a missile control surface with freeplay using the describing function method. Lee, et al.[5] applied the describing function method to analyze the flutter characteristics of the F-18 aircraft. They considered a nonlinearity of the type represented by a bilinear spring at the wing-fold hinge. They also considered free-play nonlinearity at the leading edge flap.

Tang, et al.[6] investigated free-play nonlinearity in the pitch degree of freedom. It was shown that free-play nonlinearities introduced LCO at speeds below the linear flutter speed. They concluded that the amplitude of LCO depended on initial conditions, airspeed, and degree of nonlinearity. Kim, et al.[7] particularly investigated same problems but with a flexible two-degree-of-freedom (2-DOF) airfoil. They performed nonlinear aeroelastic analyses for both the fre-

*Corresponding author. Tel.: +98-21-77791044.
*E-mail address:* irani@kntu.ac.ir

 doi: 10.1016/S1000-9361(11)60032-0

quency domain and time domain. Dessi, et al.[8] constructed a theoretical model with a 3-DOF aeroelastic typical section with a trailing-edge control surface including cubic nonlinear springs for both the nonlinear description of the torsional stiffness and of the hinge elastic moment. The equations of motion are then analyzed by a singular perturbation technique based on the normal-form method. The nonlinear response of a structurally nonlinear airfoil in subsonic flow has similarly been the subject of a number of investigations such as works done by Conner[9] and Tang[10], et al. for discontinuous structural nonlinearities , and by O'Neil[11] and Sheta[12], et al. for continuous structural nonlinearities.

The nonlinear flutter behavior may have a benign and explosive flutter nature. In the former case, above the linear flutter speed, the system tends to be stable LCO, leading to a supercritical pitchfork-like Hopf bifurcation as depicted in Fig.1(a), whereas in the second case which is demonstrated in Fig.1(b), even below the linear flutter speed, the system may experience instability, namely a subcritical knee-like Hopf bifurcation. At the Hopf point equilibrium solution or stable zero amplitude response converts to the periodic solution, and the amplitude of the unstable LCO becomes zero contrary to the stable one. Also at the turning/fold point when the initial conditions are sufficiently high, the unstable LCO becomes stable and vice versa.

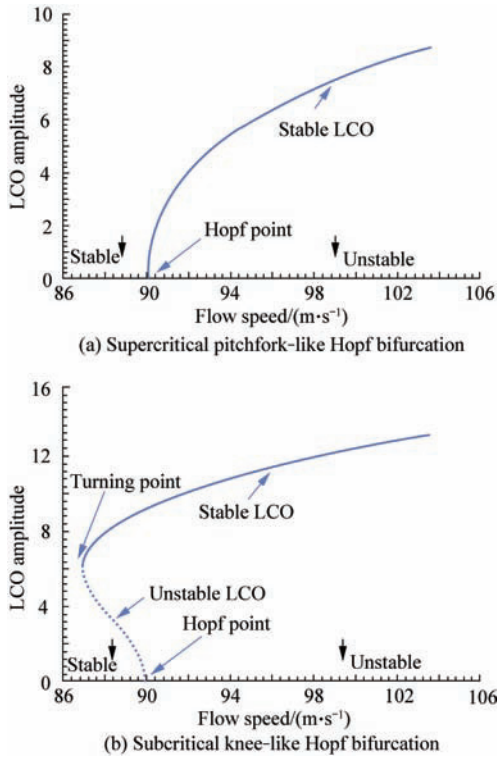


Fig.1 Two different types of Hopf bifurcation.

Harmonic balance (HB) method is used to determine the turning point (TP) location respect to the free-stream flow velocity and it is an efficient method to illustrate unstable LCO before the Hopf point, which in this case is equal to the linear flutter speed.

Cubic nonlinearity in the pitch degree of freedom causes subcritical knee-like and supercritical pitchfork-like shape Hopf bifurcation respect to the characteristics of the airfoil. On the contrary when the cubic nonlinearity exists in the flap/aileron rotation individually, one always encounters divergent flutter after the flutter speed with soft cubic nonlinearity in the control surface.

The present paper considers the governing aeroelastic equations of a 3-DOF airfoil containing cubic structural nonlinearity, either hardening or softening in the pitch degree of freedom are derived through incompressible unsteady aerodynamics, and they are studied in the time domain. The standard LCO analyses in the neighborhood of the flutter speed with both the first and third order of HB method is applied in order to evaluate the TP location and predict LCO amplitude and frequency of the airfoil. Also the results of HB method are compared with the exact numerical solution which is derived from the stable LCO. Finally, by combining the numerical and HB methods, supercritical and subcritical bifurcations within the range of an airfoil variable are identified.

## 2. Deriving Governing Equations

Consider a 3-DOF airfoil, elastically supported by a linear plunge spring and a nonlinear torsional spring. It is equipped with a control surface (flap) constrained to the wing with a linear torsional spring as shown in Fig.2. Using standard notation, the plunging deflection is denoted by $h$; $\alpha$ is the pitch angle about the elastic axis, positive in the downward direction and with nose up, and $\beta$ is the flap angle, positive when the trailing edge (TE) surface is moved down. The elastic axis is located at a distance $a_h b$ from the mid-chord, where $b$ is half the chord, while the wing mass center is located at a distance $x_\alpha b$ from the elastic axis. The axis of rotation for the flap is located at a distance $c_h b$ from the mid-chord, while the flap mass center is located at a distance $x_\beta b$ from the flap hinge. All distances are positive when measured towards the TE of the airfoil. In Fig.2, $K_\alpha$, $K_h$ and $K_\beta$ are the stiffnesses in plunge, pitch and flap, respectively.

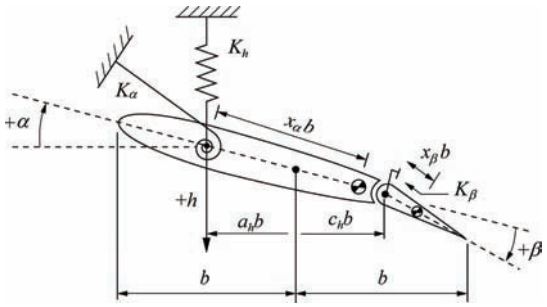


Fig.2 Schematic of 3-DOF model of a typical section.

The aeroelastic equations of motion for nonlinear 3-D typical section with a TE flap in the absence of external excitation forces can be written as follows[8]:

$$\begin{cases} -L=m\ddot{h}+S_\alpha\ddot{\alpha}+S_\beta\ddot{\beta}+C_h\dot{h}+K_hG(h) \\ M_\alpha=S_\alpha\ddot{h}+[I_\beta+b(c_h-a_h)S_\beta]\ddot{\beta}+I_\alpha\ddot{\alpha}+C_\alpha\dot{\alpha}+K_\alpha M_\alpha(\alpha) \\ M_\beta=[I_\beta+b(c_h-a_h)S_\beta]\ddot{\alpha}+S_\beta\ddot{h}+I_\beta\ddot{\beta}+C_\beta\dot{\beta}+K_\beta M_\beta(\beta) \end{cases} \tag{1}$$

where $L$ is the aerodynamic lift of wing; $m$ the total mass of airfoil; $G(h)$ nonlinear plunge stiffness terms, $M_\alpha$ and $M_\beta$ are the pitching moments about elastic axis and flap hinge; $S_\alpha$ and $S_\beta$ the airfoil static moments about the elastic axis and flap hinge; $I_\alpha$ and $I_\beta$ the airfoil mass moments of inertia about elastic axis and flap hinge; $C_h$, $C_\alpha$ and $C_\beta$ the damping coefficients in plunge, pitch and flap; $M_\alpha(\alpha)$ and $M_\beta(\beta)$ the nonlinear pitch and flap stiffness terms.

Specify the following non-dimensional coefficients by their definitions:

$$\begin{cases} x_i=\dfrac{S_i}{bm},\ \zeta_i=\dfrac{C_i}{2\sqrt{I_iK_i}},\ \ r_i=\left(\dfrac{I_i}{mb^2}\right)^{1/2} \\ \omega_i=\left(\dfrac{K_i}{I_i}\right)^{1/2}\qquad (i=\alpha,\beta) \\ \xi=\dfrac{h}{b},\ \ K_\xi=K_h,\ \ \zeta_\xi=\dfrac{C_h}{2\sqrt{mK_\xi}} \\ \omega_\xi=\left(\dfrac{K_\xi}{m}\right)^{1/2},\ \ \mu=\dfrac{m}{\rho\pi b^2} \\ U^*=\dfrac{U}{b\omega_\alpha},\ \ \tau=\dfrac{Ut}{b}=U^*\omega_\alpha t \\ \Omega_1=\dfrac{\omega_\xi}{\omega_\alpha},\ \ \Omega_2=\dfrac{\omega_\beta}{\omega_\alpha} \end{cases}$$

where $U$ is the free-steam velocity, and $\rho$ the density of air.

When the above non-dimensional coefficients are substituted in Eq.(1), the dimensionless equations of motion can be obtained

$$\begin{cases} -\dfrac{L}{mb\omega_\alpha^2U^{*2}}=\xi''+x_\alpha\alpha''+x_\beta\beta''+2\zeta_\xi\dfrac{\Omega_1}{U^*}\xi'+\dfrac{\Omega_1^2}{U^{*2}}G(\xi) \\ \dfrac{M_\alpha}{mb^2r_\alpha^2\omega_\alpha^2U^{*2}}=\dfrac{x_\alpha}{r_\alpha^2}\xi''+\dfrac{M_\alpha(\alpha)}{U^{*2}}+2\zeta_\alpha\dfrac{1}{U^*}\alpha'+\alpha''+\dfrac{r_\beta^2+(c_h-a_h)x_\beta}{r_\alpha^2}\beta'' \\ \dfrac{M_\beta}{mb^2r_\beta^2\omega_\beta^2U^{*2}}=\dfrac{x_\beta}{r_\beta^2}\xi''+\beta''+2\zeta_\beta\dfrac{\Omega_2}{U^*}\beta'+\dfrac{\Omega_2^2}{U^{*2}}M_\beta(\beta)+\dfrac{r_\beta^2+(c_h-a_h)x_\beta}{r_\beta^2}\alpha'' \end{cases} \tag{2}$$

where $(\ )'$ represents the derivative with respect to non-dimensional time $\tau$, and is used in the rest of this paper.

The aerodynamic forces are presented as follows[13]:

$$\begin{cases} L(\tau)=\rho U^{*2}b^3\omega_\alpha^2\pi\left(\alpha'+\xi''-a_h\alpha''-\dfrac{T_4}{\pi}\beta'-\dfrac{T_1}{\pi}\beta''+2W(\tau)\right) \\ M_\alpha(\tau)=-\rho U^{*2}b^4\omega_\alpha^2\pi\left[(0.5-a_h)\alpha'+\left(\dfrac{1}{8}+a_h^2\right)\alpha''+\dfrac{T_4+T_{10}}{\pi}\beta-\dfrac{T_7+(c_h-a_h)T_1}{\pi}\beta''+\dfrac{T_1-T_8-(c_h-a_h)T_4+0.5T_{11}}{\pi}\beta'-a_h\xi''-2(0.5+a_h)W(\tau)\right] \\ M_\beta(\tau)=-\rho U^{*2}b^4\omega_\alpha^2\pi\left[-\dfrac{2T_9+T_1+(0.5-a_h)T_4}{\pi}\alpha'+2\dfrac{T_{13}}{\pi}\alpha''+\dfrac{T_5-T_4T_{10}}{\pi^2}\beta-\dfrac{T_4T_{11}}{2\pi^2}\beta'-\dfrac{T_3}{\pi^2}\beta''-\dfrac{T_1}{\pi}\xi''+\dfrac{T_{12}}{\pi}W(\tau)\right] \end{cases} \tag{3}$$

where the coefficients $T_1$, $T_2$, $\cdots$, $T_{14}$ are introduced by Theodorsen[14] and given in Appendix A. Also $W(\tau)$ in terms of Wagner's function is given by

$$W(\tau)=\left[\alpha(0)+\xi'(0)+(0.5-a_h)\alpha'(0)+\frac{T_{10}}{\pi}\beta(0)+\frac{T_{11}}{2\pi}\beta'(0)\right]\varphi(\tau)+\int_0^\tau\left\{\varphi(\tau-\sigma)\left[\xi''(\sigma)+(0.5-a_h)\cdot\alpha''(\sigma)+\alpha'(\sigma)+\frac{T_{10}}{\pi}\beta'(\sigma)+\frac{T_{11}}{2\pi}\beta''(\sigma)\right]\right\}\mathrm{d}\sigma \tag{4}$$

In Eq.(4), $\varphi(\tau)$, defined as Wagner function, can be approximated as

$$\varphi(\tau)=(1-\psi_1\mathrm{e}^{-\varepsilon_1\tau}-\psi_2\mathrm{e}^{-\varepsilon_2\tau}) \tag{5}$$

where the constants $\psi_1$=0.165, $\varepsilon_1$=0.045 5, $\psi_2$=0.335, and $\varepsilon_2$=0.3 are borrowed from Jones[15].

Due to the existence of the integral terms in the integro-differential Eq.(4), it is cumbersome to integrate them numerically. A simpler set of equations was derived by Lee, et al.[16], and they introduced four new variables, so by adding the control surface, we extend the variables to six as

$$\begin{cases} w_1=\int_0^\tau\mathrm{e}^{-\varepsilon_1(\tau-\sigma)}\xi(\sigma)\mathrm{d}\sigma \Rightarrow w_1'=\xi(\tau)-\varepsilon_1w_1 \\ w_2=\int_0^\tau\mathrm{e}^{-\varepsilon_2(\tau-\sigma)}\xi(\sigma)\mathrm{d}\sigma \Rightarrow w_2'=\xi(\tau)-\varepsilon_2w_2 \\ w_3=\int_0^\tau\mathrm{e}^{-\varepsilon_1(\tau-\sigma)}\alpha(\sigma)\mathrm{d}\sigma \Rightarrow w_3'=\alpha(\tau)-\varepsilon_1w_3 \\ w_4=\int_0^\tau\mathrm{e}^{-\varepsilon_2(\tau-\sigma)}\alpha(\sigma)\mathrm{d}\sigma \Rightarrow w_4'=\alpha(\tau)-\varepsilon_2w_4 \\ w_5=\int_0^\tau\mathrm{e}^{-\varepsilon_1(\tau-\sigma)}\beta(\sigma)\mathrm{d}\sigma \Rightarrow w_5'=\beta(\tau)-\varepsilon_1w_5 \\ w_6=\int_0^\tau\mathrm{e}^{-\varepsilon_2(\tau-\sigma)}\beta(\sigma)\mathrm{d}\sigma \Rightarrow w_6'=\beta(\tau)-\varepsilon_2w_6 \end{cases} \tag{6}$$

By integrating and employing the above variables, $W(\tau)$ can be obtained as

$$\begin{aligned}W(\tau)=&[(1-\psi_1-\psi_2)+(0.5-a_h)(\psi_1\varepsilon_1+\psi_2\varepsilon_2)]\alpha(\tau)+\\&(0.5-a_h)(1-\psi_1-\psi_2)\alpha'(\tau)+(\psi_1\varepsilon_1+\psi_2\varepsilon_2)\xi(\tau)+\\&(1-\psi_1-\psi_2)\xi'(\tau)+\left[\frac{T_{10}}{\pi}(1-\psi_1-\psi_2)+\right.\\&\left.\frac{T_{11}}{2\pi}(\psi_1\varepsilon_1+\psi_2\varepsilon_2)\right]\beta(\tau)+\frac{T_{11}}{2\pi}(1-\psi_1-\psi_2)\beta'(\tau)-\\&\psi_1\varepsilon_1^2\,w_1-\psi_2\varepsilon_2^2\,w_2+\psi_1\varepsilon_1[1-(0.5-a_h)\varepsilon_1]w_3+\\&\psi_2\varepsilon_2[1-(0.5-a_h)\varepsilon_2]w_4+\frac{1}{\pi}\psi_1\varepsilon_1\left(T_{10}-\frac{T_{11}}{2}\varepsilon_1\right)w_5+\\&\frac{1}{\pi}\psi_2\varepsilon_2\left(T_{10}-\frac{T_{11}}{2}\varepsilon_2\right)w_6-\left[(0.5-a_h)\alpha(0)-\xi(0)-\right.\\&\left.\frac{T_{11}}{2\pi}\beta(0)\right](\psi_1\varepsilon_1\mathrm{e}^{-\varepsilon_1\tau}+\psi_2\varepsilon_2\mathrm{e}^{-\varepsilon_2\tau})\end{aligned}\tag{7}$$

By substituting Eq.(7) into Eq.(3), the general form of aeroelastic equations in the absence of external forces, we obtain

$$\begin{cases}f(\tau)=c_a\xi''+c_b\alpha''+c_c\beta''+c_1\xi+c_2\xi'+c_3\alpha+\\\qquad c_4\alpha'+c_5\beta+c_6\beta'+c_7w_1+c_8w_2+\\\qquad c_9w_3+c_{10}w_4+c_{11}w_5+c_{12}w_6+c_{13}\\g(\tau)=d_a\xi''+d_b\alpha''+d_c\beta''+d_1\xi+d_2\xi'+d_3\alpha+\\\qquad d_4\alpha'+d_5\beta+d_6\beta'+d_7w_1+d_8w_2+\\\qquad d_9w_3+d_{10}w_4+d_{11}w_5+d_{12}w_6+d_{13}\\h(\tau)=e_a\xi''+e_b\alpha''+e_c\beta''+e_1\xi+e_2\xi'+e_3\alpha+\\\qquad e_4\alpha'+e_5\beta+e_6\beta'+e_7w_1+e_8w_2+\\\qquad e_9w_3+e_{10}w_4+e_{11}w_5+e_{12}w_6+e_{13}\end{cases}\tag{8}$$

where coefficients $c_i$, $d_i$, $e_i$ ($i$=$a$, $b$, $c$) and $c_j$, $d_j$, $e_j$ ($j$=1, 2, ⋯, 12) are given in Appendix B. $f(\tau)$, $g(\tau)$ and $h(\tau)$ are functions of initial conditions and terms in the Wagner function. The right hand side of Eq.(8) can be written as

$$\begin{cases}f(\tau)=\left[\frac{2}{\mu}\left(\frac{1}{2}-a_h\right)\alpha(0)+\frac{2}{\mu}\xi(0)+\right.\\\qquad\left.\frac{T_{11}}{\mu\pi}\beta(0)\right](\psi_1\varepsilon_1\mathrm{e}^{-\varepsilon_1\tau}+\psi_2\varepsilon_2\mathrm{e}^{-\varepsilon_2\tau})\\g(\tau)=-\left[\frac{(1+2a_h)(0.5-a_h)}{\mu r_\alpha^2}\alpha(0)+\right.\\\qquad\left.\frac{(1+2a_h)}{\mu r_\alpha^2}\xi(0)+\frac{T_{11}(1+2a_h)}{2\mu\pi\, r_\alpha^2}\beta(0)\right]\cdot\\\qquad(\psi_1\varepsilon_1\mathrm{e}^{-\varepsilon_1\tau}+\psi_2\varepsilon_2\mathrm{e}^{-\varepsilon_2\tau})\\h(\tau)=\left[\frac{T_{12}(0.5-a_h)}{\mu\pi r_\beta^2}\alpha(0)+\frac{T_{12}}{\mu\pi r_\beta^2}\xi(0)+\right.\\\qquad\left.\frac{T_{12}T_{11}}{2\mu r_\beta^2\pi^2}\beta(0)\right](\psi_1\varepsilon_1\mathrm{e}^{-\varepsilon_1\tau}+\psi_2\varepsilon_2\mathrm{e}^{-\varepsilon_2\tau})\end{cases}\tag{9}$$

## 3. Numerical Simulation

The governing aeroelastic equations in the time domain, Eq.(8), can easily be rewritten as a set of first order ordinary differential equations (ODEs). By a suitable transformation, the resulting set of twelve ODEs is given as follows:

$$\frac{\mathrm{d}\boldsymbol{X}}{\mathrm{d}\tau}=F(\boldsymbol{X},\tau)\tag{10}$$

By assuming the following variables

$$\begin{cases}x_1=\xi,x_2=\xi',x_3=\alpha,x_4=\alpha'\\x_5=\beta,x_6=\beta',x_7=w_1,x_8=w_2\\x_9=w_3,x_{10}=w_4,x_{11}=w_5,x_{12}=w_6\end{cases}\tag{11}$$

vector $\boldsymbol{X}$ takes the following form:

$$\boldsymbol{X}=[x_2\ \ x_4\ \ x_6\ \ x_1\ \ x_3\ \ x_5\ \ x_7\ \ x_8\ \ x_9\ \ x_{10}\ \ x_{11}\ \ x_{12}]^{\mathrm{T}}\tag{12}$$

The initial conditions of the system can be expressed as

$$\begin{aligned}\boldsymbol{X}(0)=&[\xi'(0)\ \ \alpha'(0)\ \ \beta'(0)\ \ \xi(0)\ \ \alpha(0)\ \ \beta(0)\\&0\ \ 0\ \ 0\ \ 0\ \ 0\ \ 0]^{\mathrm{T}}\end{aligned}\tag{13}$$

The first ODEs in the state space form are given as

$$\begin{cases}x_1'=x_2,\ \ x_2'=-\begin{vmatrix}P&c_b&c_c\\Q&d_b&d_c\\H&e_b&e_c\end{vmatrix}\Big/\begin{vmatrix}c_a&c_b&c_c\\d_a&d_b&d_c\\e_a&e_b&e_c\end{vmatrix}\\x_3'=x_4,\ \ x_4'=-\begin{vmatrix}c_a&P&c_c\\d_a&Q&d_c\\e_a&H&e_c\end{vmatrix}\Big/\begin{vmatrix}c_a&c_b&c_c\\d_a&d_b&d_c\\e_a&e_b&e_c\end{vmatrix}\\x_5'=x_6,\ \ x_6'=-\begin{vmatrix}c_a&c_b&P\\d_a&d_b&Q\\e_a&e_b&H\end{vmatrix}\Big/\begin{vmatrix}c_a&c_b&c_c\\d_a&d_b&d_c\\e_a&e_b&e_c\end{vmatrix}\\x_7'=x_1-\varepsilon_1x_7,\ \ x_8'=x_1-\varepsilon_2x_8\\x_9'=x_3-\varepsilon_1x_9,\ \ x_{10}'=x_3-\varepsilon_2x_{10}\\x_{11}'=x_5-\varepsilon_1x_{11},\ \ x_{12}'=x_5-\varepsilon_2x_{12}\end{cases}\tag{14}$$

where

$$\begin{cases}P=c_1x_1+c_2x_2+c_3x_3+c_4x_4+c_5x_5+\\\qquad c_6x_6+c_7x_7+c_8x_8+c_9x_9+c_{10}x_{10}+\\\qquad c_{11}x_{11}+c_{12}x_{12}+c_{13}-f(\tau)\\Q=d_1x_1+d_2x_2+d_3x_3+d_4x_4+d_5x_5+\\\qquad d_6x_6+d_7x_7+d_8x_8+d_9x_9+d_{10}x_{10}+\\\qquad d_{11}x_{11}+d_{12}x_{12}+d_{13}-g(\tau)\\H=e_1x_1+e_2x_2+e_3x_3+e_4x_4+e_5x_5+\\\qquad e_6x_6+e_7x_7+e_8x_8+e_9x_9+e_{10}x_{10}+\\\qquad e_{11}x_{11}+e_{12}x_{12}+e_{13}-h(\tau)\end{cases}\tag{15}$$

The standard fourth-order Runge-Kutta method can be used to integrate the system of Eq.(10) under given initial conditions as mentioned.

## 4. Computing Linear Flutter Speed

Substituting $G(\xi)=\xi$, $M(\alpha)=\alpha$, $M(\beta)=\beta$ into Eq.(10) yields

$$\boldsymbol{X}' = \boldsymbol{A}^{-1}\boldsymbol{F} - \boldsymbol{A}^{-1}\boldsymbol{B}\boldsymbol{X} \tag{16}$$

where $\boldsymbol{A}$, $\boldsymbol{B}$ are 12 by 12 and $\boldsymbol{F}$ is 12 by 1 sparse matrices given in Appendix C.

The linear flutter velocity $U_{\mathrm{L}}^{*}$ is obtained by solving the resultant eigenvalue problem. Stability of the linear system depends on the eigenvalues of $-\boldsymbol{A}^{-1}\boldsymbol{B}$ in Eq.(16). Solution of this equation gives twelve eigenvalues; six with zero imaginary parts and three sets of complex conjugate pairs. By increasing non-dimensional speed, the first positive or asymmetrically zero real part of some of the eigenvalues indicates instability speed due to the fact that positive damping requires the system to keep stable. The corresponding imaginary part equals reduced frequency $k$ ($k=\omega/(U^{*}\omega_{\alpha})$, $\omega$ is the fundamental frequency of the motion) where the system exhibits oscillatory behavior for non-zero values of reduced frequency. So the non-zero imaginary part indicates flutter speed, with positive real part; the eigenvalue with zero imaginary part represents divergence speed, with positive real part.

For a representative sample, by assuming the characteristics of the airfoil as below:

$$\Omega_1 = 1.2,\ r_\alpha = 0.5,\ \mu = 100,\ x_\alpha = 0.25,\ r_\beta = 0.097\,1$$
$$x_\beta = 0.012\,5,\ c_h = 0.6,\ a_h = -0.5,\ \Omega_2 = 3.5$$

Fig.3 shows the variation of the real part of the complex conjugate pairs with non-dimensional velocity ($U^{*}$). At low velocities all the eigenvalues have negative real parts, indicating that the system is stable. However, as $U^{*}$ is increased, the real part of one of the complex conjugate pairs increases and eventually becomes positive at $U_{\mathrm{L}}^{*}$=4.663 031.

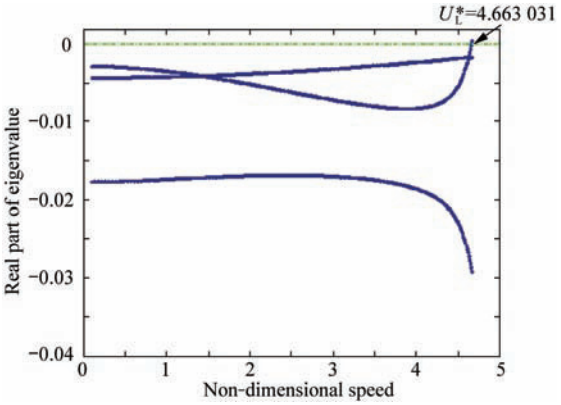


Fig.3 Real part of eigenvalues as a function of non-dimensional speed.

## 5. The First Order HB (HB1) Method

The HB method is an efficient method for the prediction of the frequency and amplitude of LCO that occurs at speeds above the linear flutter speed for wings containing a cubic nonlinearity. In order to apply this method, plunge and pitch motions should assume the form of a trigonometric series, such as Fourier series. So, the time-dependent part of plunge and pitch motions can be approximated as

$$\begin{cases} \xi(\tau) = f_1 \sin(\omega\tau) + g_1 \cos(\omega\tau) \\ \alpha(\tau) = a_1 \sin(\omega\tau) \\ \beta(\tau) = h_1 \sin(\omega\tau) + n_1 \cos(\omega\tau) \end{cases} \tag{17}$$

Define cubic structural nonlinearity in pitch, plunge and control surface rotation of the airfoil as

$$\begin{cases} G(\xi) = \beta_\xi \xi + \beta_{\xi^3}\xi^3 \\ M(\alpha) = \beta_\alpha \alpha + \beta_{\alpha^3}\alpha^3 \\ M(\beta) = \beta_\beta \beta + \beta_{\beta^3}\beta^3 \end{cases} \tag{18}$$

where $\beta_\alpha$ and $\beta_{\alpha^3}$, $\beta_\beta$ and $\beta_{\beta^3}$, and $\beta_\xi$ and $\beta_{\xi^3}$ are constants in nonlinear terms $M_\alpha(\alpha)$, $M_\beta(\beta)$ and $M_\xi(\xi)$, respectively.

Substituting Eq.(17) into Eq.(6) and Eq.(8), and calculating the coefficients of $\sin(\omega\tau)$ and $\cos(\omega\tau)$, we obtain the system $a_1, f_1, g_1, h_1, n_1$ and $\omega$:

$$\begin{cases} m_1 a_1 + p_1 f_1 + q_1 g_1 + s_1 h_1 + u_1 n_1 + \\ \quad \dfrac{3}{4}\left(\dfrac{\Omega_1}{U^*}\right)^2 \beta_{\xi^3} f_1 (f_1^2 + g_1^2) = 0 \\ m_2 a_1 + p_2 f_1 + q_2 g_1 + s_2 h_1 + u_2 n_1 + \\ \quad \dfrac{3}{4}\left(\dfrac{\Omega_1}{U^*}\right)^2 \beta_{\xi^3} g_1 (f_1^2 + g_1^2) = 0 \\ m_3 a_1 + p_3 f_1 + q_3 g_1 + s_3 h_1 + u_3 n_1 + \\ \quad \dfrac{3}{4}\left(\dfrac{1}{U^*}\right)^2 \beta_{\alpha^3} a_1^3 = 0 \\ m_4 a_1 + p_4 f_1 + q_4 g_1 + s_4 h_1 + u_4 n_1 = 0 \\ m_5 a_1 + p_5 f_1 + q_5 g_1 + s_5 h_1 + u_5 n_1 + \\ \quad \dfrac{3}{4}\left(\dfrac{\Omega_2}{U^*}\right)^2 \beta_{\beta^3} h_1 (h_1^2 + n_1^2) = 0 \\ m_6 a_1 + p_6 f_1 + q_6 g_1 + s_6 h_1 + u_6 n_1 + \\ \quad \dfrac{3}{4}\left(\dfrac{\Omega_2}{U^*}\right)^2 \beta_{\beta^3} n_1 (h_1^2 + n_1^2) = 0 \end{cases} \tag{19}$$

where $m_i$, $p_i$, $q_i$, $s_i$ and $u_i$ ($i$=1, 2, ⋯, 6) are functions of system parameters and frequency $\omega$, and their definitions are given in Appendix D. For velocities larger than the bifurcation value, the motions have limited-amplitude, i.e. there exist non-zero solutions to Eq.(19).

At the particular case where we only have cubic

nonlinearity in the pitch degree of freedom or $\beta_{\alpha^3}\neq 0$, $\beta_{\beta^3}=0$, $\beta_{\xi^3}=0$, the determinant of five equations of Eq.(19) should be zero. We can obtain acceptable frequency by the following equation:

$$\begin{vmatrix} m_1 & m_2 & m_4 & m_5 & m_6 \\ p_1 & p_2 & p_4 & p_5 & p_6 \\ q_1 & q_2 & q_4 & q_5 & q_6 \\ s_1 & s_2 & s_4 & s_5 & s_6 \\ u_1 & u_2 & u_4 & u_5 & u_6 \end{vmatrix}=0 \tag{20}$$

In this instance for the supercritical bifurcation, it yields two acceptable $\omega$ as well as zero frequency for the equilibrium solution. Once the frequency is obtained $f_1$, $g_1$, $h_1$ and $n_1$can be solved from the four relations of Eq.(19) in terms of $a_1$, that is

$$f_1=-a_1\begin{vmatrix} m_1 & m_2 & m_5 & m_6 \\ q_1 & q_2 & q_5 & q_6 \\ s_1 & s_2 & s_5 & s_6 \\ u_1 & u_2 & u_5 & u_6 \end{vmatrix}\Big/\begin{vmatrix} p_1 & p_2 & p_5 & p_6 \\ q_1 & q_2 & q_5 & q_6 \\ s_1 & s_2 & s_5 & s_6 \\ u_1 & u_2 & u_5 & u_6 \end{vmatrix}=a_1F_1$$

$$g_1=+a_1\begin{vmatrix} m_1 & m_2 & m_5 & m_6 \\ p_1 & p_2 & p_5 & p_6 \\ s_1 & s_2 & s_5 & s_6 \\ u_1 & u_2 & u_5 & u_6 \end{vmatrix}\Big/\begin{vmatrix} p_1 & p_2 & p_5 & p_6 \\ q_1 & q_2 & q_5 & q_6 \\ s_1 & s_2 & s_5 & s_6 \\ u_1 & u_2 & u_5 & u_6 \end{vmatrix}=a_1G_1$$

$$h_1=-a_1\begin{vmatrix} m_1 & m_2 & m_5 & m_6 \\ p_1 & p_2 & p_5 & p_6 \\ q_1 & q_2 & q_5 & q_6 \\ u_1 & u_2 & u_5 & u_6 \end{vmatrix}\Big/\begin{vmatrix} p_1 & p_2 & p_5 & p_6 \\ q_1 & q_2 & q_5 & q_6 \\ s_1 & s_2 & s_5 & s_6 \\ u_1 & u_2 & u_5 & u_6 \end{vmatrix}=a_1H_1$$

$$n_1=+a_1\begin{vmatrix} m_1 & m_2 & m_5 & m_6 \\ p_1 & p_2 & p_5 & p_6 \\ q_1 & q_2 & q_5 & q_6 \\ s_1 & s_2 & s_5 & s_6 \end{vmatrix}\Big/\begin{vmatrix} p_1 & p_2 & p_5 & p_6 \\ q_1 & q_2 & q_5 & q_6 \\ s_1 & s_2 & s_5 & s_6 \\ u_1 & u_2 & u_5 & u_6 \end{vmatrix}=a_1N_1 \tag{21}$$

Substituting Eq.(21) into the third equation of Eq.(19) yields the pitch, plunge and flap amplitude:

$$\begin{cases} \text{Pitch amplitude/rad:} \\ a_1=2U^*\sqrt{-\dfrac{m_3+p_3F_1+q_3G_1+s_3H_1+u_3N_1}{3\beta_{\alpha^3}}} \\ \text{Plunge amplitude:} \\ \sqrt{f_1^2+g_1^2}=a_1\sqrt{F_1^2+G_1^2} \\ \text{Flap amplitude/rad:} \\ \sqrt{h_1^2+n_1^2}=a_1\sqrt{H_1^2+N_1^2} \end{cases} \tag{22}$$

## 6. The Third Order HB (HB3) Method

The second dominant harmonic is associated with a frequency of $3\omega$. For a higher order approximation in the analytical prediction, we rewrite Eq.(17) as

$$\begin{cases} \xi(\tau)=f_1\sin(\omega\tau)+g_1\cos(\omega\tau)+f_3\sin(3\omega\tau)+ \\ \qquad g_3\cos(3\omega\tau) \\ \alpha(\tau)=a_1\sin(\omega\tau)+a_3\sin(3\omega\tau)+b_3\cos(3\omega\tau) \\ \beta(\tau)=h_1\sin(\omega\tau)+n_1\cos(\omega\tau)+h_3\sin(3\omega\tau)+ \\ \qquad n_3\cos(3\omega\tau) \end{cases} \tag{23}$$

At the particular case where $\beta_{\alpha^3}\neq 0$, $\beta_{\beta^3}=0$, $\beta_{\xi^3}=0$, substituting Eq.(23) into Eq.(6) and Eq.(8), and calculating the coefficients of $\sin(\omega\tau)$ and $\cos(\omega\tau)$, we obtain the system of $a_1, f_1, g_1, h_1, n_1, a_3, b_3, f_3, g_3, h_3, n_3$ and $\omega$:

$$\begin{cases} m_1a_1+p_1f_1+q_1g_1+s_1h_1+u_1n_1=0 \\ m_2a_1+p_2f_1+q_2g_1+s_2h_1+u_2n_1=0 \\ m_3a_1+p_3f_1+q_3g_1+s_3h_1+u_3n_1+\dfrac{3}{4}\left(\dfrac{1}{U^*}\right)^2\cdot \\ \quad \beta_{\alpha^3}(-a_1^2a_3+a_1^3+2a_1a_3^2+2a_1b_3^2)=0 \\ m_4a_1+p_4f_1+q_4g_1+s_4h_1+u_4n_1-\dfrac{3}{4}\left(\dfrac{1}{U^*}\right)^2\beta_{\alpha^3}a_1^2b_3=0 \\ m_5a_1+p_5f_1+q_5g_1+s_5h_1+u_5n_1=0 \\ m_6a_1+p_6f_1+q_6g_1+s_6h_1+u_6n_1=0 \\ m_{13}a_3+v_{13}b_3+p_{13}f_3+q_{13}g_3+s_{13}h_3+u_{13}n_3=0 \\ m_{23}a_3+v_{23}b_3+p_{23}f_3+q_{23}g_3+s_{23}h_3+u_{23}n_3=0 \\ m_{33}a_3+v_{33}b_3+p_{33}f_3+q_{33}g_3+s_{33}h_3+u_{33}n_3+ \\ \quad \dfrac{3}{4}\left(\dfrac{1}{U^*}\right)^2\beta_{\alpha^3}(a_3b_3^2+2a_1^2a_3-a_1^3/3+a_3^3)=0 \\ m_{43}a_3+v_{43}b_3+p_{43}f_3+q_{43}g_3+s_{43}h_3+u_{43}n_3+ \\ \quad \dfrac{3}{4}\left(\dfrac{1}{U^*}\right)^2\beta_{\alpha^3}(a_3^2b_3+2a_1^2b_3+b_3^3)=0 \\ m_{53}a_3+v_{53}b_3+p_{53}f_3+q_{53}g_3+s_{53}h_3+u_{53}n_3=0 \\ m_{63}a_3+v_{63}b_3+p_{63}f_3+q_{63}g_3+s_{63}h_3+u_{63}n_3=0 \end{cases} \tag{24}$$

where $m_{i3}$, $p_{i3}$, $v_{i3}$, $q_{i3}$, $s_{i3}$, $u_{i3}$ ($i$=1, 2, ⋯, 6) are functions of system parameters and frequency $\omega$, and their expressions are given in Appendix D. Also variables $m_i$, $p_i$, $q_i$, $s_i$ and $u_i$ ($i$=1, 2, ⋯, 6) are the same as mentioned in HB1 method.

The variables $f_1$, $g_1$, $h_1$, $n_1$ in terms of $a_1$ can be solved from the four expressions in Eq.(24), and their solutions are the same as Eq.(21). Also the variables $f_3$, $g_3$, $h_3$, $n_3$ can be solved from another four expressions in Eq.(24) in terms of $a_3$ and $b_3$:

$$\begin{cases} f_3 = -\left( a_3 \begin{vmatrix} m_{13} & m_{23} & m_{53} & m_{63} \\ q_{13} & q_{23} & q_{53} & q_{63} \\ s_{13} & s_{23} & s_{53} & s_{63} \\ u_{13} & u_{23} & u_{53} & u_{63} \end{vmatrix} + b_3 \begin{vmatrix} v_{13} & v_{23} & v_{53} & v_{63} \\ q_{13} & q_{23} & q_{53} & q_{63} \\ s_{13} & s_{23} & s_{53} & s_{63} \\ u_{13} & u_{23} & u_{53} & u_{63} \end{vmatrix} \right) \Bigg/ \begin{vmatrix} p_{13} & p_{23} & p_{53} & p_{63} \\ q_{13} & q_{23} & q_{53} & q_{63} \\ s_{13} & s_{23} & s_{53} & s_{63} \\ u_{13} & u_{23} & u_{53} & u_{63} \end{vmatrix} = F_{3a}a_3 + F_{3b}b_3 \\ g_3 = +\left( a_3 \begin{vmatrix} m_{13} & m_{23} & m_{53} & m_{63} \\ p_{13} & p_{23} & p_{53} & p_{63} \\ s_{13} & s_{23} & s_{53} & s_{63} \\ u_{13} & u_{23} & u_{53} & u_{63} \end{vmatrix} + b_3 \begin{vmatrix} v_{13} & v_{23} & v_{53} & v_{63} \\ p_{13} & p_{23} & p_{53} & p_{63} \\ s_{13} & s_{23} & s_{53} & s_{63} \\ u_{13} & u_{23} & u_{53} & u_{63} \end{vmatrix} \right) \Bigg/ \begin{vmatrix} p_{13} & p_{23} & p_{53} & p_{63} \\ q_{13} & q_{23} & q_{53} & q_{63} \\ s_{13} & s_{23} & s_{53} & s_{63} \\ u_{13} & u_{23} & u_{53} & u_{63} \end{vmatrix} = G_{3a}a_3 + G_{3b}b_3 \\ h_3 = -\left( a_3 \begin{vmatrix} m_{13} & m_{23} & m_{53} & m_{63} \\ p_{13} & p_{23} & p_{53} & p_{63} \\ q_{13} & q_{23} & q_{53} & q_{63} \\ u_{13} & u_{23} & u_{53} & u_{63} \end{vmatrix} + b_3 \begin{vmatrix} v_{13} & v_{23} & v_{53} & v_{63} \\ p_{13} & p_{23} & p_{53} & p_{63} \\ q_{13} & q_{23} & q_{53} & q_{63} \\ u_{13} & u_{23} & u_{53} & u_{63} \end{vmatrix} \right) \Bigg/ \begin{vmatrix} p_{13} & p_{23} & p_{53} & p_{63} \\ q_{13} & q_{23} & q_{53} & q_{63} \\ s_{13} & s_{23} & s_{53} & s_{63} \\ u_{13} & u_{23} & u_{53} & u_{63} \end{vmatrix} = H_{3a}a_3 + H_{3b}b_3 \\ n_3 = +\left( a_3 \begin{vmatrix} m_{13} & m_{23} & m_{53} & m_{63} \\ p_{13} & p_{23} & p_{53} & p_{63} \\ q_{13} & q_{23} & q_{53} & q_{63} \\ s_{13} & s_{23} & s_{53} & s_{63} \end{vmatrix} + b_3 \begin{vmatrix} v_{13} & v_{23} & v_{53} & v_{63} \\ p_{13} & p_{23} & p_{53} & p_{63} \\ q_{13} & q_{23} & q_{53} & q_{63} \\ s_{13} & s_{23} & s_{53} & s_{63} \end{vmatrix} \right) \Bigg/ \begin{vmatrix} p_{13} & p_{23} & p_{53} & p_{63} \\ q_{13} & q_{23} & q_{53} & q_{63} \\ s_{13} & s_{23} & s_{53} & s_{63} \\ u_{13} & u_{23} & u_{53} & u_{63} \end{vmatrix} = N_{3a}a_3 + N_{3b}b_3 \end{cases} \tag{25}$$

So the other four expressions of Eq.(24) become

$$\begin{cases} M_3 a_1 + \dfrac{3}{4}\left(\dfrac{1}{U^*}\right)^2 \beta_{\alpha^3}(-a_1^2 a_3 + a_1^3 + 2a_1 a_3^2 + 2a_1 b_3^2) = 0 \\ M_4 a_1 - \dfrac{3}{4}\left(\dfrac{1}{U^*}\right)^2 \beta_{\alpha^3} a_1^2 b_3 = 0 \\ M_{33} a_3 + N_{33} b_3 + \dfrac{3}{4}\left(\dfrac{1}{U^*}\right)^2 \beta_{\alpha^3}\left(a_3 b_3^2 + 2a_1^2 a_3 - \dfrac{a_1^3}{3} + a_3^3\right) = 0 \\ M_{43} a_3 + N_{43} b_3 + \dfrac{3}{4}\left(\dfrac{1}{U^*}\right)^2 \beta_{\alpha^3}(a_3^2 b_3 + 2a_1^2 b_3 + b_3^3) = 0 \end{cases} \tag{26}$$

where

$$\begin{cases} M_3 = m_3 + p_3 F_1 + q_3 G_1 + s_3 H_1 + u_3 N_1 \\ M_4 = m_4 + p_4 F_1 + q_4 G_1 + s_4 H_1 + u_4 N_1 \\ M_{33} = m_{33} + p_{33} F_{3a} + q_{33} G_{3a} + s_{33} H_{3a} + u_{33} N_{3a} \\ N_{33} = v_{33} + p_{33} F_{3b} + q_{33} G_{3b} + s_{33} H_{3b} + u_{33} N_{3b} \\ M_{43} = -N_{33} = m_{43} + p_{43} F_{3a} + q_{43} G_{3a} + s_{43} H_{3a} + u_{43} N_{3a} \\ N_{43} = M_{33} = v_{43} + p_{43} F_{3b} + q_{43} G_{3b} + s_{43} H_{3b} + u_{43} N_{3b} \end{cases} \tag{27}$$

Ref.[17] solved a equation similar to Eq.(26) for a 2-DOF airfoil without control surface after some complicated algebraic manipulations. Taking advantage of the suggested relations, we have

$$\begin{aligned} 0 = {} & M_4^5 - 8M_4^4 M_{43} + M_4^3(10M_{43}^2 + 4M_{33}^2 + M_3^2 - 4M_{33}M_3) + M_4^2(30M_{43}M_{33}M_3 - 9M_{43}M_{33}^2 - \\ & 12M_{43}M_3^2 - 24M_{43}^2) + M_4(36M_{43}^2 M_3^2 - 30M_{43}^2 M_{33}M_3 + \\ & 9M_{43}^4 + 9M_{43}^2 M_{33}^2) + 3M_{43}^3 M_3^2 \end{aligned} \tag{28}$$

$$\begin{cases} a_1^2 = \dfrac{U^{*2}}{\beta_{\alpha^3}} \cdot \dfrac{4M_{43}(M_3 M_{43} + M_4 M_{33})}{M_4^2 - 4M_3 M_{43} - 3M_{43}^2} \\ a_3^2 + b_3^2 = \dfrac{U^{*2}}{\beta_{\alpha^3}} \cdot \dfrac{4M_{43}(M_3 M_4 + M_4 M_{33})}{3(M_4^2 - 4M_3 M_{43} - 3M_{43}^2)} \end{cases} \tag{29}$$

By using Eq.(28), we can obtain acceptable frequency, then by substituting Eq.(29) into the two expressions of Eq.(26), $a_1$, $a_3$ and $b_3$ could be found. Consequently, from Eq.(21) and Eq.(25), we can derive the specific values of $f_1$, $g_1$, $h_1$, $n_1$ and $f_3$, $g_3$, $h_3$, $n_3$ respectively.

## 7. Determining TP Location

TP exists only in subcritical bifurcations where the amplitude of the unstable and stable LCOs, as well as frequency, becomes equal to each other. In a 3-DOF airfoil with cubic nonlinearity, the characteristics of the airfoil and the sign of pitch cubic nonlinearity affect the location of TP irrespective of its magnitude and initial conditions.

In this section by utilizing HB1 method, we investigative how the characteristics of the airfoil affected by the location of TP and how the subcritical bifurcation converts to supercritical one or vice versa. To be simplified, HB1 method is applied in order to find TP lo-

cation. The results are consistent with that obtained by HB3 method.

The variation of airfoil parameters is depicted in Fig.4 by using the characteristics of the airfoil, as defined in previous section, and applying hardening cubic nonlinearity as $\beta_{\alpha^3}>0$, $\beta_{\beta^3}=0$, $\beta_{\xi^3}=0$, $\beta_\alpha=\beta_\beta=\beta_\xi=1$. By increasing $a_h$, supercritical bifurcation converts to the subcritical at $a_h=-0.46$, which causes the TP location to move farther away from the Hopf point. Also in the range of $0.05\leq c_h<0.41$, there exists subcritical bifurcation and increasing this parameter causes the TP to come closer to the Hopf point. In another instance, in the range $127<\mu<194.5$, by increasing $\mu$ initially, TP comes closer to the Hopf point, only to leap suddenly away where the type of bifurcation becomes supercritical with no TP. Other parameters, such as $x_\alpha$, $r_\alpha$ and $\Omega_1$, are also illustrated in Fig.4, and their variation can be expressed similarly. Within this range for all plots in Fig.4, the instability speed is flutter speed as the response of the dynamical system is investigated. Higher values for $a_h$ up to the level of −0.1 are not considered in this analysis as they change the instability speed to divergence one.

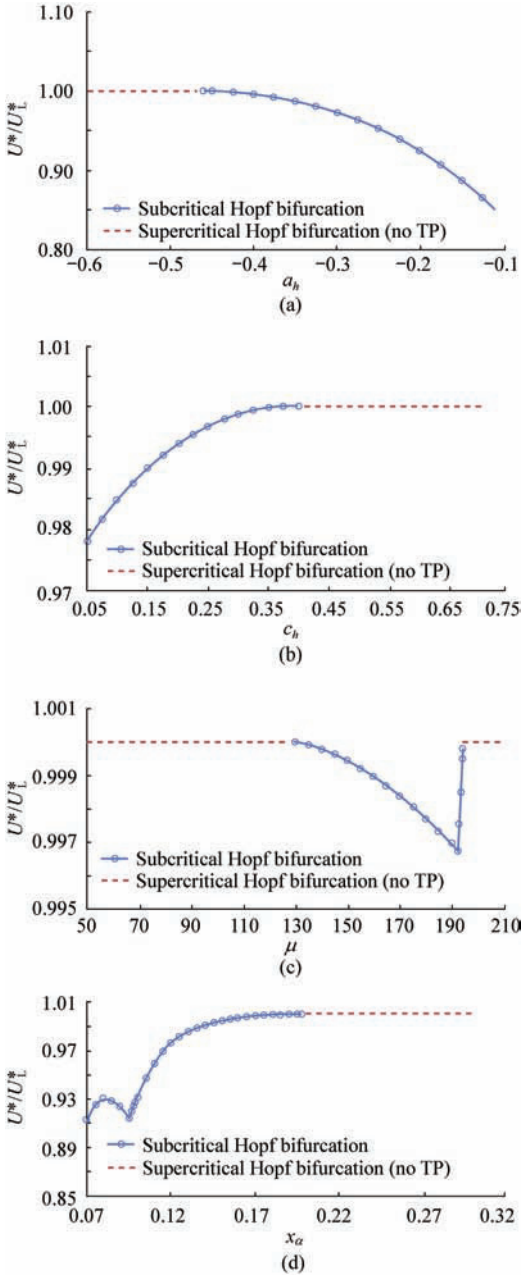


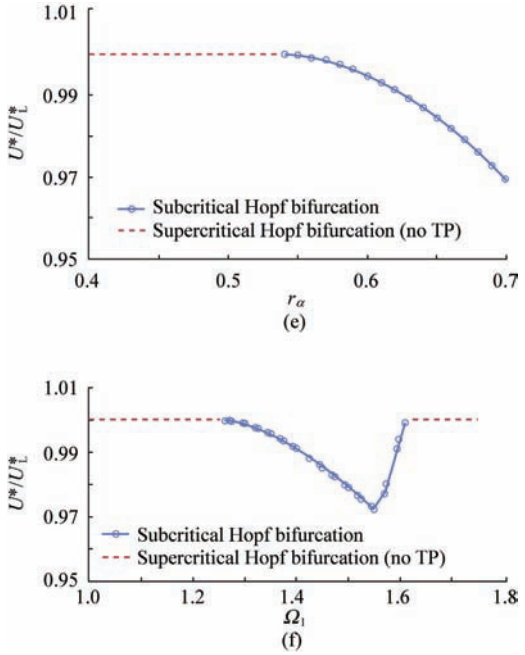


Fig.4 TP location with respect to variation of $a_h$, $c_h$, $\mu$, $x_\alpha$, $r_\alpha$ and $\Omega_1$ in an airfoil with $\Omega_1=1.2$, $r_\alpha=0.5$, $\mu=100$, $x_\alpha=0.25$, $\Omega_2=3.5$, $r_\beta=0.079\ 1$, $x_\beta=0.012\ 5$, $c_h=0.6$, $a_h=-0.5$, $G(\xi)=\xi$, $M(\beta)=\beta$, $\beta_{\alpha^3}>0$, $\beta_\alpha=1$.

## 8. Bifurcation Plots

### 8.1. Cubic hardening stiffness

Supercritical bifurcation emerges when an airfoil with the characteristics mentioned in Section 6, including cubic hardening stiffness in the pitch degree of freedom, is considered. Also by changing the level of $a_h$ to −0.4, the bifurcation becomes subcritical with TP=0.996 16 $U^*/U_L^*$ where the structural nonlinearity is in the form of

$$G(\xi)=\xi,\quad M(\beta)=\beta,\ M(\alpha)=\alpha+50\alpha^3$$

Now, by using the HB1 and HB3 methods, the finite limited amplitude of the stable and unstable LCOs are computed and depicted in Fig.5. Also to verify the results, stable LCO for a variation of $U^*/U_L^*$ are numerically evaluated and except for control surface or flap amplitude, the results of HB methods show good agreement with the numerical solution. HB1 method could not predict the shape of oscillations perfectly in the flap amplitude, due to the specific shape of LCO where the oscillations are not combination of $\sin(\omega\tau)$ and $\cos(\omega\tau)$ individually.

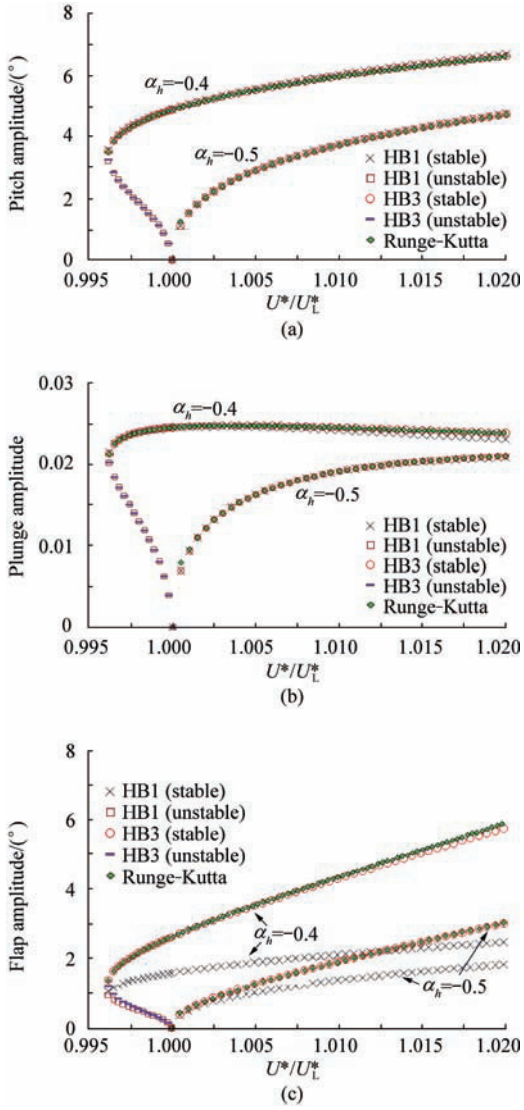


Fig.5 Bifurcation plots for pitch, plunge and flap amplitudes for an airfoil with $\Omega_1$=1.2, $r_\alpha$=0.5, $\mu$=100, $x_\alpha$= 0.25, $\Omega_2$=3.5, $r_\beta$= 0.097 1, $x_\beta$= 0.012 5, $c_h$=0.6, $a_h$= –0.4, –0.5, $G(\xi)=\xi$, $M(\beta)=\beta$, $M(\alpha)=\alpha+50\alpha^3$.

In Fig.6, stable LCOs for a location before Hopf bifurcation and after that by HB3 and Runge-Kutta approaches for flap oscillations with $a_h$= –0.4 are plotted. Note that the phase difference between two oscillations by two methods is not important because the HB method starts plotting of the LCOs at $\tau$=0.

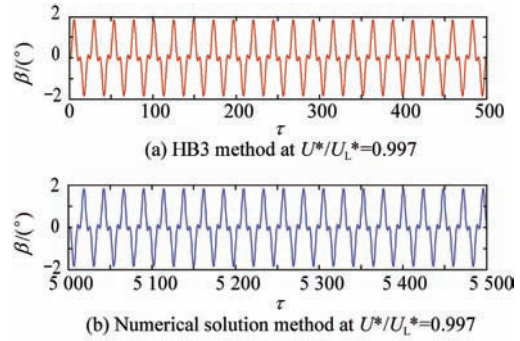


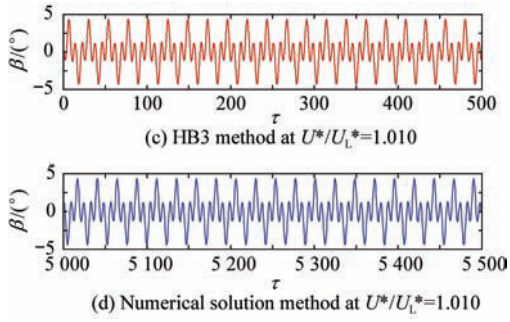


Fig.6 Stable LCO vs non-dimensional time for an airfoil with $\Omega_1$=1.2, $r_\alpha$= 0.5, $\mu$=100, $x_\alpha$= 0.25, $\Omega_2$=3.5, $r_\beta$= 0.097 1, $x_\beta$= 0.012 5, $c_h$=0.6, $a_h$= –0.4, $G(\xi)=\xi$, $M(\beta)=\beta$, $M(\alpha)=\alpha+50\alpha^3$.

### 8.2. Cubic softening stiffness

By similar procedure like Section 8.1 but for $\beta_{\alpha^3}$ = –50, the subcritical bifurcation occurs this time for $a_h$= –0.5 with TP=0.998 6 $U^*/U_L^*$. In Fig.7 the bifurca-

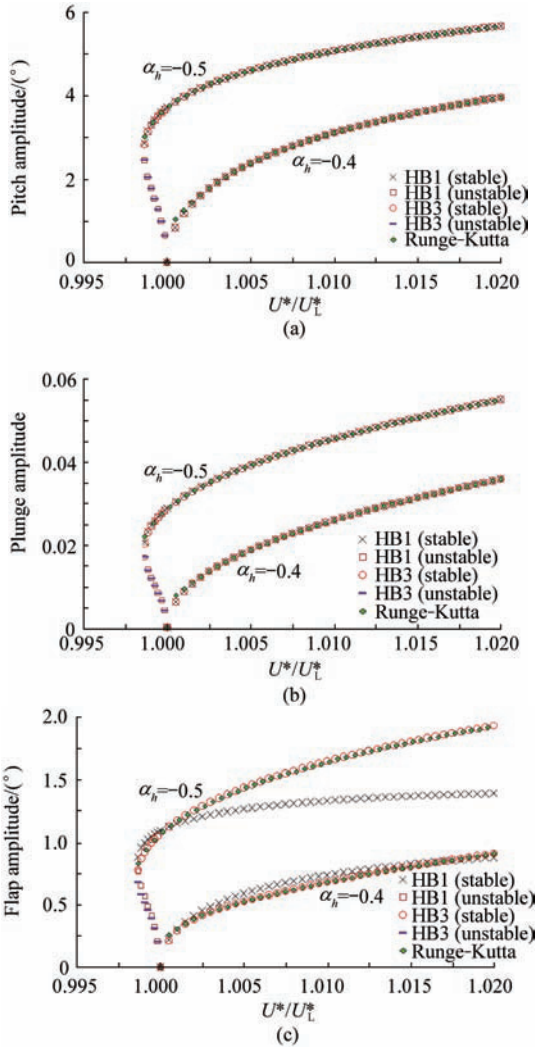


Fig.7 Bifurcation plots for pitch, plunge and flap amplitudes for an airfoil with $\Omega_1$=1.2, $r_\alpha$= 0.5, $\mu$=100, $x_\alpha$= 0.25, $\Omega_2$=3.5, $r_\beta$= 0.097 1, $x_\beta$= 0.012 5, $c_h$= 0.6, $a_h$= –0.4, –0.5, $G(\xi)=\xi$, $M(\beta)=\beta$, $M(\alpha)=\alpha-50\alpha^3$.

tion for two sets of parameters of $a_h$ is plotted. Substantial difference between HB1 and HB3 methods, and Runge-Kutta method for the flap amplitude was already explored in Section 8.1.

In Fig.8, stable LCOs for a location before Hopf bifurcation and after that by HB3 and Runge-Kutta approaches for flap oscillations with $a_h$= –0.5 are plotted. The phase difference is unimportant in this case as explained before.

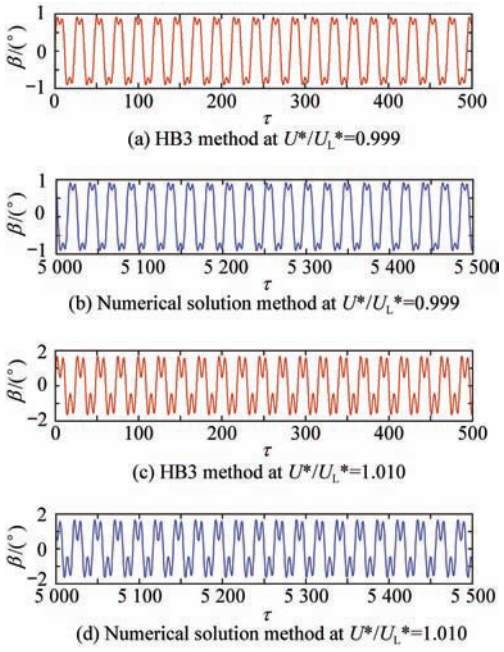


Fig.8 Sable LCO vs non-dimensional time for an airfoil with $\Omega_1$=1.2, $r_\alpha$=0.5, $\mu$=100, $x_\alpha$=0.25, $\Omega_2$=3.5, $r_\beta$= 0.097 1, $x_\beta$= 0.012 5, $c_h$=0.6, $a_h$= –0.5, $G(\xi)=\xi$, $M(\beta)=\beta$, $M(\alpha)=\alpha-50\alpha^3$.

In a 2-DOF airfoil (without control surface) with cubic softening stiffness in pitch degree of freedom, even below the linear flutter speed, we encounter divergent oscillations with respect to initial conditions. This issue is also correct for a 3-DOF airfoil with cubic softening stiffness in the control surface. But in the present format, divergent oscillations are encountered occasionally based on the initial conditions.

By combining the numerical and HB methods, types of bifurcation such as supercritical and subcritical bifurcations as well as divergent flutter area by variation of $a_h$ are identified in two cases for $\Omega_1$=1.2 and $\Omega_1$=1.0. In the subcritical bifurcation when initial conditions are not sufficiently large, the response will be damped or backed to the equilibrium state. Otherwise, aeroelastic response leads to either stable LCOs or divergent oscillations.

In Figs.9-10, divergent oscillations/flutter, LCO and equilibrium state/solution areas are obtained through numerical solution and the boundary of two types of bifurcations with each other or with damped oscillations area (i.e. TPs curve) are designated by HB1 method.

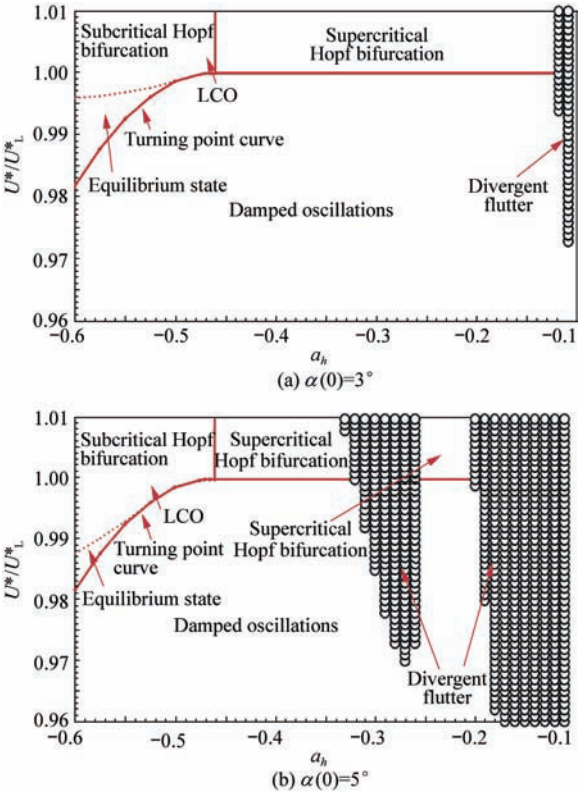


Fig.9 Types of bifurcations and oscillations by variation of $a_h$ for an airfoil with $\Omega_1$=1.2, $r_\alpha$=0.5, $\mu$=100, $x_\alpha$= 0.25, $\Omega_2$=3.5, $r_\beta$= 0.097 1, $x_\beta$= 0.012 5, $c_h$= 0.6, $G(\xi)=\xi$, $M(\beta)=\beta$, $M(\alpha)=\alpha-50\alpha^3$, $\beta(0)=\xi(0)=\alpha'(0)=\xi'(0)=\beta'(0)=0$.

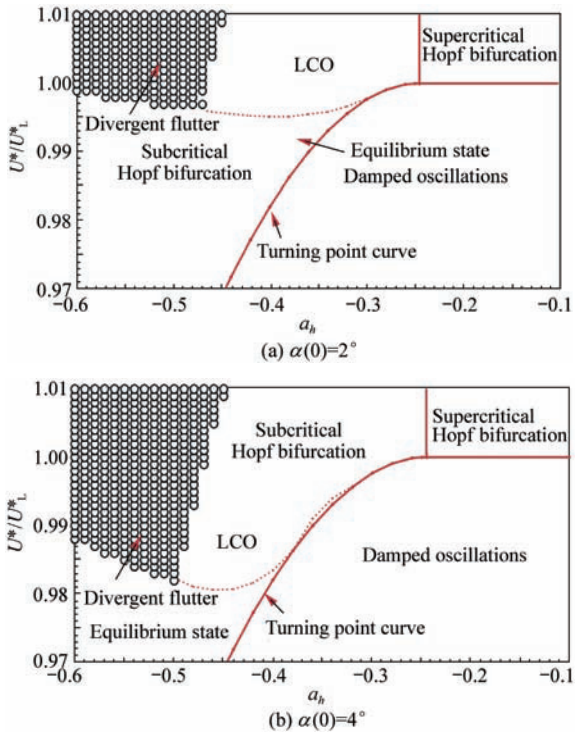


Fig.10 Types of bifurcations and oscillations by variation of $a_h$ for an airfoil with $\Omega_1$=1, $r_\alpha$=0.5, $\mu$=100, $x_\alpha$= 0.25, $\Omega_2$=3.5, $r_\beta$= 0.097 1, $x_\beta$= 0.012 5, $c_h$= 0.6, $G(\xi)=\xi$, $M(\beta)=\beta$, $M(\alpha)=\alpha-50\alpha^3$, $\beta(0)=\xi(0)=\alpha'(0)=\xi'(0)=\beta'(0)=0$.

In Figs.9(a)-9(b), with $\Omega_1$=1.2 the only non-zero initial conditions are $\alpha(0)$=3° and $\alpha(0)$=5° respectively. The stronger initial disturbance causes larger divergent and LCO area. For another sample in Figs.10(a)-10(b), with $\Omega_1$=1 the only non-zero initial conditions are $\alpha(0)$=2° and $\alpha(0)$=4° respectively. So the system excited with small initial disturbances usually does not lead to divergent oscillations.

## 9. Conclusions

In this work, the governing aeroelastic equations of a 3-DOF airfoil in an incompressible flow are derived in the time domain. The nonlinear aeroelastic behavior of the 3-DOF airfoil with hardening and softening cubic nonlinearities in pitch degree of freedom is also studied in the time domain, and the prediction of LCO amplitude and frequency by using the HB method and numerical solution is investigated and the results are illustrated in a series of bifurcation plots. The following outcomes are concluded:

(1) The bifurcation diagram is very dependant on the position of the elastic center.

(2) The type of bifurcation and TP location depends on the characteristics of the airfoil as well as the parameters of structural nonlinearity.

(3) For cubic softening stiffness in pitch degree freedom in a 3-DOF airfoil, whether the type of bifurcations is subcritical or supercritical, and the initial conditions may cause divergent oscillations.

HB method is in a good agreement with Runge-Kutta method, but for flap amplitude of HB1 method it could not predict the shape of oscillations contrary to the higher order of this semi-analytical method.

## References


[1] Woolston D S, Runyan H L, Andrews R E. An investigation of effects of certain types of structural nonlinearities on wing and control surface flutter. Journal of Aeronautical Science 1957; 24(1): 57-63.

[2] Shen S F. An approximate analysis of nonlinear flutter problems. Journal of Aerospace Science 1959; 26(1): 25-32.

[3] Breitbach E J. Effect of structural nonlinearities on aircraft vibration and flutter. 45th Structures and Materials AGARD Panel Meeting. 1977.

[4] Laurenson R M, Trn R M. Flutter analysis of missile control surface containing structural nonlinearities. AIAA Journal 1980; 18(10): 1245-1251.

[5] Lee B H K, Tron A. Effects of structural nonlinearities on flutter characteristics of the CF-18 aircraft. Journal of Aircraft 1989; 26(8): 781-786.

[6] Tang D M, Dowell E H. Flutter and stall response of a helicopter blade with structural nonlinearity. Journal of Aircraft 1992; 29(5): 953-960.

[7] Kim S H, Lee I. Aeroelastic analysis of a flexible airfoil with a freeplay nonlinearity. Journal of Sound and Vibration 1996; 193(4): 823-846.

[8] Dessi D, Mastroddi F. Limit-cycle stability reversal via singular perturbation and wing-flap flutter. Journal of Fluids and Structures 2004; 19(6): 765-783.

[9] Conner M D, Tang D M, Dowell E H, et al. Nonlinear behaviour of a typical airfoil section with a control surface freeplay: a numerical and experimental study. Journal of Fluids and Structures 1997; 11(1): 89-109.

[10] Tang D, Dowell E H, Virgin L N. Limit cycle behavior of an airfoil with a control surface. Journal of Fluids and Structures 1998; 12(7): 839-858.

[11] O'Neil T, Strganac T W. Aeroelastic response of a rigid wing supported by nonlinear springs. Journal of Aircraft 1998; 35(4): 616-622.

[12] Sheta E F, Harrand V J, Thompson D E, et al. Computational and experimental investigation of limit cycle oscillations of nonlinear aeroelastic systems. AIAA-2000-1399, 2000.

[13] Bisplinghoff R L, Ashley H, Halfman R L. Aeroelasticity. Reading, MA, USA: Addison-Wesley Publication Company, 1955.

[14] Theodorsen T. General theory of aerodynamic instability and the mechanism of flutter. NACA Report 496, 1935.

[15] Jones R T. The unsteady lift of a wing of finite aspect ratio. NACA Report 681, 1940.

[16] Lee B H K, Gong L, Wong Y S. Analysis and computation of nonlinear dynamic response of a two-degree-of freedom system and its application in aeroelasticity. Journal of Fluids and Structures 1997; 11(3): 225-246.

[17] Lee B H K, Liub L, Chung K W. Airfoil motion in subsonic flow with strong cubic nonlinear restoring forces. Journal of Sound and Vibration 2005; 281(3-5): 699-717.


## Biography:


**Saied IRANI** Born in 1966, he received his B.S. degree from Sharif University of Technology (Tehran, Iran) in 1989. He then received his M.S. and Ph.D. degrees from University of New South Wales (Sydney, Australia) in 1994 and 2000 respectively. He is currently an assistant professor in K. N. Toosi University of Technology. His main research interests are aeroelasticity and multi-scale analysis.
E-mail: irani@kntu.ac.ir


## Appendix A: Coefficients for Eq.(3)

$$T_1 = -\frac{1}{3}\sqrt{1-c_h^2}\,(2+c_h^2) + c_h \arccos c_h$$

$$T_2 = c_h(1-c_h^2) - \sqrt{1-c_h^2}\,(1+c_h^2)\arccos c_h + c_h(\arccos c_h)^2$$

$$T_3 = -\left(\frac{1}{8}+c_h^2\right)(\arccos c_h)^2 + \frac{1}{4}c_h^2\sqrt{1-c_h^2}\,(7+2c_h^2)\cdot \arccos c_h - \frac{1}{8}(1-c_h^2)(5c_h^2+4)$$

$$T_4 = -\arccos c_h + c_h\sqrt{1-c_h^2}$$

$$T_5 = -(1-c_h^2) - (\arccos c_h)^2 + 2c_h\sqrt{1-c_h^2}\arccos c_h$$

$$T_6 = T_2$$

$$T_7 = -\left(\frac{1}{8}+c_h^2\right)\arccos c_h + \frac{1}{8}c_h\sqrt{1-c_h^2}\,(7+2c_h^2)$$

$$T_8 = -\frac{1}{3}\sqrt{1-c_h^2}\,(2c_h^2+1) + c_h \arccos c_h$$

$$T_9 = \frac{1}{2}\left[\frac{1}{3}\sqrt{1-c_h^2}\,(1-c_h^2) + a_h T_4\right]$$

$$T_{10}=\sqrt{1-c_h^2}+\arccos c_h$$

$$T_{11}=(1-2c_h)\arccos c_h+\sqrt{1-c_h^2}(2-c_h)$$

$$T_{12}=\sqrt{1-c_h^2}(2+c_h)-(2c_h+1)\arccos c_h$$

$$T_{13}=-\frac{1}{2}[T_7+(c_h-a_h)T_1]$$

$$T_{14}=\frac{1}{16}+\frac{1}{2}a_hc_h$$

## Appendix B: Coefficients for Eq.(8) and Eq.(15)

$$c_a=1+\frac{1}{\mu},\quad c_b=x_\alpha-\frac{a_h}{\mu},\quad c_c=x_\beta-\frac{T_1}{\mu\pi}$$

$$c_1=\frac{2}{\mu}(\psi_1\varepsilon_1+\psi_2\varepsilon_2),\quad c_2=2\zeta_\xi\frac{\Omega_1}{U^*}+\frac{2}{\mu}(1-\psi_1-\psi_2)$$

$$c_3=\frac{2}{\mu}\left[(1-\psi_1-\psi_2)+\left(\frac{1}{2}-a_h\right)(\psi_1\varepsilon_1+\psi_2\varepsilon_2)\right]$$

$$c_4=\frac{1+2(0.5-a_h)(1-\psi_1-\psi_2)}{\mu}$$

$$c_5=\frac{T_{11}}{\mu\pi}(\psi_1\varepsilon_1+\psi_2\varepsilon_2)+\frac{2T_{10}}{\mu\pi}(1-\psi_1-\psi_2)$$

$$c_6=\frac{T_{11}}{\mu\pi}(1-\psi_1-\psi_2)-\frac{T_4}{\mu\pi}$$

$$c_7=-\frac{2\psi_1\varepsilon_1^2}{\mu},\quad c_8=-\frac{2\psi_2\varepsilon_2^2}{\mu}$$

$$c_9=\frac{2\psi_1\varepsilon_1[1-(0.5-a_h)\varepsilon_1]}{\mu}$$

$$c_{10}=\frac{2\psi_2\varepsilon_2[1-(0.5-a_h)\varepsilon_2]}{\mu}$$

$$c_{11}=\frac{\psi_1\varepsilon_1}{\mu\pi}(2T_{10}-T_{11}\varepsilon_1)$$

$$c_{12}=\frac{\psi_2\varepsilon_2}{\mu\pi}(2T_{10}-T_{11}\varepsilon_2),\quad c_{13}=\frac{\Omega_1^2}{U^{*2}}G(\xi)$$

$$d_a=\frac{x_\alpha}{r_\alpha^2}-\frac{a_h}{\mu r_\alpha^2},\quad d_b=1+\frac{\frac{1}{8}+a_h^2}{\mu r_\alpha^2}$$

$$d_c=\frac{r_\beta^2+(c_h-a_h)x_\beta}{r_\alpha^2}-\frac{T_7+(c_h-a_h)T_1}{\mu\pi r_\alpha^2}$$

$$d_1=-\frac{(1+2a_h)(\psi_1\varepsilon_1+\psi_2\varepsilon_2)}{\mu r_\alpha^2}$$

$$d_2=-\frac{(1+2a_h)(1-\psi_1-\psi_2)}{\mu r_\alpha^2}$$

$$d_3=-\frac{(2a_h+1)(1-\psi_1-\psi_2)}{\mu r_\alpha^2}-\frac{(1+2a_h)(1-2a_h)(\psi_1\varepsilon_1+\psi_2\varepsilon_2)}{2\mu r_\alpha^2}$$

$$d_4=2\zeta_\alpha\frac{1}{U^*}+\frac{1-2a_h}{2\mu r_\alpha^2}-\frac{(1+2a_h)(1-2a_h)(1-\psi_1-\psi_2)}{2\mu r_\alpha^2}$$

$$d_5=\frac{T_4+T_{10}}{\mu\pi r_\alpha^2}-\frac{(1+2a_h)T_{10}(1-\psi_1-\psi_2)}{\mu\pi r_\alpha^2}-\frac{(1+2a_h)T_{11}(\psi_1\varepsilon_1+\psi_2\varepsilon_2)}{2\mu\pi r_\alpha^2}$$

$$d_6=\frac{T_1-T_8-(c_h-a_h)T_4+\frac{T_{11}}{2}}{\mu\pi r_\alpha^2}-\frac{(1+2a_h)T_{11}(1-\psi_1-\psi_2)}{2\mu\pi r_\alpha^2}$$

$$d_7=\frac{(1+2a_h)\psi_1\varepsilon_1^2}{\mu r_\alpha^2},\quad d_8=\frac{(1+2a_h)\psi_2\varepsilon_2^2}{\mu r_\alpha^2}$$

$$d_9=-\frac{(1+2a_h)\psi_1\varepsilon_1[1-(0.5-a_h)\varepsilon_1]}{\mu r_\alpha^2}$$

$$d_{10}=-\frac{(1+2a_h)\psi_2\varepsilon_2[1-(0.5-a_h)\varepsilon_2]}{\mu r_\alpha^2}$$

$$d_{11}=-\frac{(1+2a_h)\psi_1\varepsilon_1\left(T_{10}-\frac{T_{11}\varepsilon_1}{2}\right)}{\mu\pi r_\alpha^2}$$

$$d_{12}=-\frac{(1+2a_h)\psi_2\varepsilon_2\left(T_{10}-\frac{T_{11}\varepsilon_2}{2}\right)}{\mu\pi r_\alpha^2}$$

$$d_{13}=\frac{M_\alpha(\alpha)}{U^{*2}}$$

$$e_a=\frac{x_\beta}{r_\beta^2}-\frac{T_1}{\mu\pi r_\beta^2}$$

$$e_b=1+\frac{(c_h-a_h)x_\beta}{r_\beta^2}+\frac{2T_{13}}{\mu\pi r_\beta^2}$$

$$e_c=1-\frac{T_3}{\mu\pi^2 r_\beta^2}$$

$$e_1=\frac{T_{12}(\psi_1\varepsilon_1+\psi_2\varepsilon_2)}{\mu\pi r_\beta^2},\quad e_2=\frac{T_{12}(1-\psi_1-\psi_2)}{\mu\pi r_\beta^2}$$

$$e_3=\frac{T_{12}}{\mu\pi r_\beta^2}(1-\psi_1-\psi_2)+\frac{T_{12}(0.5-a_h)}{\mu\pi r_\beta^2}(\psi_1\varepsilon_1+\psi_2\varepsilon_2)$$

$$e_4=-\frac{T_1+2T_9+(0.5-a_h)T_4}{\mu\pi r_\beta^2}+\frac{T_{12}(0.5-a_h)(1-\psi_1-\psi_2)}{\mu\pi r_\beta^2}$$

$$e_5=\frac{T_5-T_4T_{10}}{\mu\pi^2 r_\beta^2}+\frac{T_{12}T_{10}(1-\psi_1-\psi_2)}{\mu r_\beta^2\pi^2}+\frac{T_{12}T_{11}(\psi_1\varepsilon_1+\psi_2\varepsilon_2)}{2\mu r_\beta^2\pi^2}$$

$$e_6=2\zeta_\beta\frac{\Omega_2}{U^*}-\frac{T_4T_{11}}{2\mu\pi^2 r_\beta^2}+\frac{T_{12}T_{11}(1-\psi_1-\psi_2)}{2\mu r_\beta^2\pi^2}$$

$$e_7=-\frac{T_{12}\psi_1\varepsilon_1^2}{\mu\pi r_\beta^2},\quad e_8=-\frac{T_{12}\psi_2\varepsilon_2^2}{\mu\pi r_\beta^2}$$

$$e_9=\frac{T_{12}\psi_1\varepsilon_1[1-(0.5-a_h)\varepsilon_1]}{\mu\pi r_\beta^2}$$

$$e_{10}=\frac{T_{12}\psi_2\varepsilon_2[1-(0.5-a_h)\varepsilon_2]}{\mu\pi r_\beta^2}$$

$$e_{11}=\frac{T_{12}\psi_1\varepsilon_1\left(T_{10}-\dfrac{T_{11}\varepsilon_1}{2}\right)}{\mu r_\beta^2\ \pi^2}$$

$$e_{12}=\frac{T_{12}\psi_2\varepsilon_2\left(T_{10}-\dfrac{T_{11}\varepsilon_2}{2}\right)}{\mu r_\beta^2\ \pi^2}$$

$$e_{13}=\frac{\Omega_2^2}{U^{*2}}M_\beta(\beta)$$

## Appendix C: Coefficients for Eq.(16)

$$\boldsymbol{A}=\begin{bmatrix}
c_a & c_b & c_c & 0 & 0 & 0 & 0 & 0 & 0 & 0 & 0 & 0\\
d_a & d_b & d_c & 0 & 0 & 0 & 0 & 0 & 0 & 0 & 0 & 0\\
e_a & e_b & e_c & 0 & 0 & 0 & 0 & 0 & 0 & 0 & 0 & 0\\
0 & 0 & 0 & 1 & 0 & 0 & 0 & 0 & 0 & 0 & 0 & 0\\
0 & 0 & 0 & 0 & 1 & 0 & 0 & 0 & 0 & 0 & 0 & 0\\
0 & 0 & 0 & 0 & 0 & 1 & 0 & 0 & 0 & 0 & 0 & 0\\
0 & 0 & 0 & 0 & 0 & 0 & 1 & 0 & 0 & 0 & 0 & 0\\
0 & 0 & 0 & 0 & 0 & 0 & 0 & 1 & 0 & 0 & 0 & 0\\
0 & 0 & 0 & 0 & 0 & 0 & 0 & 0 & 1 & 0 & 0 & 0\\
0 & 0 & 0 & 0 & 0 & 0 & 0 & 0 & 0 & 1 & 0 & 0\\
0 & 0 & 0 & 0 & 0 & 0 & 0 & 0 & 0 & 0 & 1 & 0\\
0 & 0 & 0 & 0 & 0 & 0 & 0 & 0 & 0 & 0 & 0 & 1
\end{bmatrix}$$

$$\boldsymbol{B}=\begin{bmatrix}
c_2 & c_4 & c_6 & c_1+\dfrac{\Omega_1^2}{U^{*2}} & c_3 & c_5 & c_7 & c_8 & c_9 & c_{10} & c_{11} & c_{12}\\
d_2 & d_4 & d_6 & d_1 & d_3+\dfrac{1}{U^{*2}} & d_5 & d_7 & d_8 & d_9 & d_{10} & d_{11} & d_{12}\\
e_2 & e_4 & e_6 & e_1 & e_3 & e_5+\dfrac{\Omega_2^2}{U^{*2}} & e_7 & e_8 & e_9 & e_{10} & e_{11} & e_{12}\\
-1 & 0 & 0 & 0 & 0 & 0 & 0 & 0 & 0 & 0 & 0 & 0\\
0 & -1 & 0 & 0 & 0 & 0 & 0 & 0 & 0 & 0 & 0 & 0\\
0 & 0 & -1 & 0 & 0 & 0 & 0 & 0 & 0 & 0 & 0 & 0\\
0 & 0 & 0 & -1 & 0 & 0 & \varepsilon_1 & 0 & 0 & 0 & 0 & 0\\
0 & 0 & 0 & -1 & 0 & 0 & 0 & \varepsilon_2 & 0 & 0 & 0 & 0\\
0 & 0 & 0 & 0 & -1 & 0 & 0 & 0 & \varepsilon_1 & 0 & 0 & 0\\
0 & 0 & 0 & 0 & -1 & 0 & 0 & 0 & 0 & \varepsilon_2 & 0 & 0\\
0 & 0 & 0 & 0 & 0 & -1 & 0 & 0 & 0 & 0 & \varepsilon_1 & 0\\
0 & 0 & 0 & 0 & 0 & -1 & 0 & 0 & 0 & 0 & 0 & \varepsilon_2
\end{bmatrix}$$

$$\boldsymbol{F}=[f(\tau)\quad g(\tau)\quad h(\tau)\quad 0\quad 0\quad 0\quad 0\quad 0\quad 0\quad 0\quad 0\quad 0]^{\mathrm{T}}$$

## Appendix D: Coefficients for Eq.(19) and Eq.(24)

$$m_1=-c_b\omega^2+c_3+c_9\varepsilon_1t_1+c_{10}\varepsilon_2t_2$$
$$m_2=c_4\omega-c_9\omega t_1-c_{10}\omega t_2$$
$$m_3=-d_b\omega^2+d_3+d_9\varepsilon_1t_1+d_{10}\varepsilon_2t_2+\beta_\alpha(1/U^*)^2$$
$$m_4=d_4\omega-d_9\omega t_1-d_{10}\omega t_2$$
$$m_5=-e_b\omega^2+e_3+e_9\varepsilon_1t_1+e_{10}\varepsilon_2t_2$$
$$m_6=e_4\omega-e_9\omega t_1-e_{10}\omega t_2$$
$$p_1=-c_a\omega^2+c_1+c_7\varepsilon_1t_1+c_8\varepsilon_2t_2+\beta_\xi(\Omega_1/U^*)^2$$
$$p_2=c_2\omega-c_7\omega t_1-c_8\omega t_2$$
$$p_3=-d_a\omega^2+d_1+d_7\varepsilon_1t_1+d_8\varepsilon_2t_2$$
$$p_4=d_2\omega-d_7\omega t_1-d_8\omega t_2$$
$$p_5=-e_a\omega^2+e_1+e_7\varepsilon_1t_1+e_8\varepsilon_2t_2$$
$$p_6=e_2\omega-e_7\omega t_1-e_8\omega t_2$$

$$q_1=-p_2,\quad q_2=p_1$$
$$q_3=-p_4,\quad q_4=p_3$$
$$q_5=-p_6,\quad q_6=p_5$$

$$s_1=-c_c\omega^2+c_5+c_{11}\varepsilon_1t_1+c_{12}\varepsilon_2t_2$$
$$s_2=c_6\omega-c_{11}\omega t_1-c_{12}\omega t_2$$
$$s_3=-d_c\omega^2+d_5+d_{11}\varepsilon_1t_1+d_{12}\varepsilon_2t_2$$
$$s_4=d_6\omega-d_{11}\omega t_1-d_{12}\omega t_2$$
$$s_5=-e_c\omega^2+e_5+e_{11}\varepsilon_1t_1+e_{12}\varepsilon_2t_2+\beta_\beta(\Omega_2/U^*)^2$$
$$s_6=e_6\omega-e_{11}\omega t_1-e_{12}\omega t_2$$

$$u_1=-s_2,\quad u_2=s_1,\quad u_3=-s_4,$$
$$u_4=s_3,\quad u_5=-s_6,\quad u_6=s_5$$

$$m_{13}=-9c_b\omega^2+c_3+c_9\varepsilon_1t_{13}+c_{10}\varepsilon_2t_{23}$$
$$m_{23}=3c_4\omega-3c_9\omega t_{13}-3c_{10}\omega t_{23}$$

$$m_{33} = -9d_b\omega^2 + d_3 + d_9\varepsilon_1 t_{13} + d_{10}\varepsilon_2 t_{23} + \beta_\alpha (1/U^*)^2$$
$$m_{43} = 3d_4\omega - 3d_9\omega t_{13} - 3d_{10}\omega t_{23}$$
$$m_{53} = -9e_b\omega^2 + e_3 + e_9\varepsilon_1 t_{13} + e_{10}\varepsilon_2 t_{23}$$
$$m_{63} = 3e_4\omega - 3e_9\omega t_{13} - 3e_{10}\omega t_{23}$$
$$p_{13} = -9c_a\omega^2 + c_1 + c_7\varepsilon_1 t_{13} + c_8\varepsilon_2 t_{23} + \beta_\xi (\Omega_1/U^*)^2$$
$$p_{23} = 3c_2\omega - 3c_7\omega t_{13} - 3c_8\omega t_{23}$$
$$p_{33} = -9d_a\omega^2 + d_1 + d_7\varepsilon_1 t_{13} + d_8\varepsilon_2 t_{23}$$
$$p_{43} = 3d_2\omega - 3d_7\omega t_{13} - 3d_8\omega t_{23}$$
$$p_{53} = -9e_a\omega^2 + e_1 + e_7\varepsilon_1 t_{13} + e_8\varepsilon_2 t_{23}$$
$$p_{63} = 3e_2 - 3e_7\omega t_{13} - 3e_8\omega t_{23}$$
$$v_{13} = -m_{23}, \quad v_{23} = m_{13}$$
$$v_{33} = -m_{43}, \quad v_{43} = m_{33}$$
$$v_{53} = -m_{63}, \quad v_{63} = m_{53}$$
$$q_{13} = -p_{23}, \quad q_{23} = p_{13}$$
$$q_{33} = -p_{43}, \quad q_{43} = p_{33}$$
$$q_{53} = -p_{63}, \quad q_{63} = p_{53}$$
$$s_{13} = -9c_c\omega^2 + c_5 + c_{11}\varepsilon_1 t_{13} + c_{12}\varepsilon_2 t_{23}$$
$$s_{23} = 3c_6\omega - 3c_{11}\omega t_{13} - 3c_{12}\omega t_{23}$$
$$s_{33} = -9d_c\omega^2 + d_5 + d_{11}\varepsilon_1 t_{13} + d_{12}\varepsilon_2 t_{23}$$
$$s_{43} = 3d_6\omega - 3d_{11}\omega t_{23} - 3d_{12}\omega t_{23}$$
$$s_{53} = -9e_c\omega^2 + e_5 + e_{11}\varepsilon_1 t_{13} + e_{12}\varepsilon_2 t_{23} + \beta_\beta (\Omega_2/U^*)^2$$
$$s_{63} = 3e_6\omega - 3e_{11}\omega t_{13} - 3e_{12}\omega t_{23}$$
$$u_{13} = -s_{23}, \quad u_{23} = s_{13}$$
$$u_{33} = -s_{43}, \quad u_{43} = s_{33}$$
$$u_{53} = -s_{63}, \quad u_{63} = s_5$$
$$t_1 = (\varepsilon_1^2 + \omega^2)^{-1}, \quad t_2 = (\varepsilon_2^2 + \omega^2)^{-1}$$
$$t_{13} = (\varepsilon_1^2 + 9\omega^2)^{-1}, \quad t_{23} = (\varepsilon_2^2 + 9\omega^2)^{-1}$$